Proceedings of ALGORITMY 2020
pp. 229–239

WATER SUSPENSION INFILTRATION WITH ADSORPTION IN UNSATURATED-SATURATED POROUS MEDIA*

JOZEF KAČUR† AND PATRIK MIHALA‡

Abstract. Transportation of contaminated water suspension (water and silt) in unsaturated-saturated porous media is considered. Moreover, the water in suspension is contaminated and this contaminant is adsorbed by the porous media matrix. The deposition of silt in the matrix is characterized by a filtration function, and the contaminant adsorption is modeled by a sorption isotherm. The mathematical model includes a coupled system for the water suspension infiltration, silt, and contaminant (uniformly mixed in the water) transport with dispersion and their deposition and adsorption in porous media. Filtration function expresses the rate of silt deposition depending on the amount of (immobile) deposited silt. Contaminant adsorption is modeled in terms of the contaminant concentration in suspension, the amount of adsorbed contaminant, and the rate of adsorption. The main goal is to develop a suitable numerical approximation that can be applied to the solution of direct and inverse problems. In the numerical experiments, we demonstrate the correctness and the effectiveness of the used method.

Key words. suspension and heat transport, heat energy exchange, silt deposition, contaminant adsorption, porous media, numerical modelling

AMS subject classifications. 65M08, 65M32, 93A30

1. Introduction. The flow of water suspension (silt particles mixed in water) in porous media was modeled and intensively discussed last decade. Silt particles are retained at the pores. Some of them become immobile and some of them continue transportation. Kinetics of particle retention depends on the concentration of particles in suspension, on the amount of already retained immobile particles and on the speed of water suspension. The retention process is much more complex, influenced also by the ionic strength of microparticles and physicochemical mechanisms including the contact with porous media. Also, repulsive interaction occurs, and thus both phenomena, deposition, and release of particles, participate. For practical applications, not all attributes and influences could be included in the model. The deposition of particles based on the mechanical mechanism modeled in terms of filtration function was presented by Herzig et all [13]. This model was simple, expressing just conservation of the mass of deposited particles and particles in suspension. There, the kinetics of particle retention is dependent on their concentration in water suspension and level of retained ones expressed in terms of the filtration function. Determination of filtration function (dependent on the amount of retained particles) was discussed in a series of papers, see [14], [11], and citations there. In spite of elegant analysis, the used method requires very special (smooth and obeying some structural conditions) input data which represent an inflow/outflow measurements of concentration. A more complex model has been discussed in [12] (see also citations there) where transport of silt solute together with particle transport was considered containing de-

*The authors confirm financial support by the Slovak Research and Development Agency under the contracts APVV-15-0681.

†Faculty of Civil Engineering, STU Bratislava, Radlinského 11, 810 05 SLOVAKIA (Jozef.Kacur@fmph.uniba.sk).

‡FMFI UK Bratislava, Department of Mathematics, Mlynská dolina, 842 48 SLOVAKIA (pmihala@gmail.com).

position/release phenomenon. The kinetics of deposition/release is expressed in terms of silt concentration and water velocity changes. Suspension flow is assumed in fully saturated porous media. The flow speed in [13] is constant and in [12] is assumed in an analytical form.
Besides the filtration property of porous media also the distribution of particle deposition in porous media is of interest.

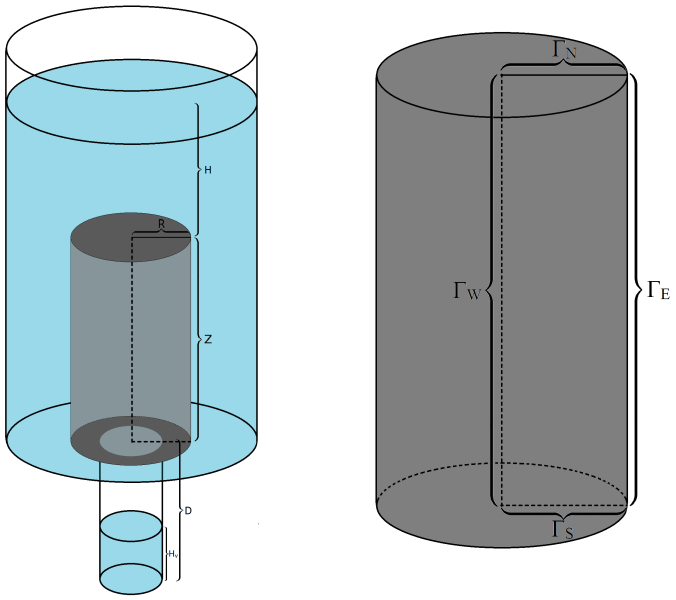

FIG. 1.1. *Sample with its cross-section*

In our contribution, we discuss a more complex 3D model for suspension flow where we allow also partial saturation. The contaminant in suspension is transported and absorbed by the matrix. Both deposited silt and adsorbed contaminant change porosity and hydraulic permeability. The suspension flow in unsaturated porous media is governed by gravitation and capillarity phenomenon which depends on suspension saturation in porous media. Thus, the complex system is strongly coupled. Mathematical models for the flow of water and contaminant transport is discussed in monographs, e.g. [8], [9], [10] and numerical modeling with inverse problems we have realized in [6] for 1D case. The governing equations of our system consist of a strongly nonlinear and degenerate elliptic-parabolic system. The suspension flow is governed by Richard's type equation where capillary pressure and hydraulic permeability versus suspension saturation is assumed in an empirical model by van Genuchten/Mualem [4]. Moreover, these fundamental flow relations and porosity depend on deposited silt, adsorbed contaminant. Here, we do not consider the heat energy transport with its change and influence on the viscosity. The heat exchange between the porous media matrix and infiltrated suspension in the pores has been analyzed in our previous contribution [15] where only clean water has been considered.

In this contribution, we consider contaminant adsorption and only silt deposition mode. Our main goal is the development of a correct and efficient numerical method for solving the direct (when all model parameters are available) and inverse problems in which we determine the adsorption isotherm and the filtration function. There,

the inflow/outflow measurements in laboratory experiments are used. In the solution of inverse problems, we consider the 3D sample in cylindrical form. The 3D sample enables us to use a large scale of experimental scenarios choosing suitable boundary conditions. We choose optimal of them with respect to the reliability of determined model parameters and the technical simplicity of realized additional measurements needed for the inverse method. The experiment is schematically drawn in Fig. 1.1.

Our numerical method is based on operator splitting and finite volume method with flexible time discretization where successively along with small-time interval we separately solve suspension flow, transport of silt, and contaminant with deposition and adsorption. In the numerical approximation of the suspension flow model we follow the strategy introduced in [3] and also used in well-known software Hydrus (see [2]).

In Section 2 we present the mathematical model and in Section 3 its transformation to the cylindrical coordinates. In Section 4 we discuss the numerical approximation of the proposed model. The solution of the inverse problems is presented in section 5. The solution of direct complex problem is introduced in Section 6 with its graphical interpretation.

2. Mathematical model.

2.1. Suspension flow model. The flow is modeled by hydraulic permeability $K = K_s k(h)$, with

$$K_s = \kappa_0 \frac{\rho g}{\mu},$$

where ρ and μ are the density and the dynamical viscosity of the suspension, respectively. The coefficient κ_0 depends only on the structure of the porous medium and g is the gravitational acceleration. Denote by θ suspension saturation, θf amount of silt in suspension, f silt fraction in the suspension, and by h the pressure head of suspension. The model function $k(h)$ is linked with the capillary forces dependent on the corresponding effective saturation $\bar{\theta}$ (see van Genuchten [4]). We note that these parameters depend on suspension deposited material $S = (S_1, S_2)$ where S_1 is adsorbed contaminant, and S_2 is deposited silt. By C_w we denote contaminant concentration in suspension. By ρ_w, ρ_s and ρ_m we denote the densities of water, silt and matrix, respectively. By κ we denote the adsorption kinetics rate coefficient. Let Ψ_1 denote the adsorption isotherm and Ψ_2 the infiltration function which will be specified below. We use $\mathbf{D}$ for dispersion matrix linked with our porous media. The flux of water suspension $\vec{q_0}$ is the global flux of water and silt together and is driven by gravitation and capillary pressure, expressed in terms of hydraulic permeability and saturation using van Genuchten-Mualem empirical model. We consider K in more general form

$$K(C_w, S, h) = \frac{(\theta_s - \theta_r - (S_1 + S_2))}{\theta_s} K_s(C_w, S, h) \cdot k(h),$$

since the deposited material decreases the original porosity θ_s. Here, $K_s = K(C_w, S, 0)$ is the hydraulic permeability in fully saturated porous media. We consider k in the van Genuchten/Mualem empirical form (see [4])

$$k(\bar{\theta}) = \bar{\theta}^{\frac{1}{2}}(1 - (1 - \bar{\theta}^{\frac{1}{m}})^m)^2 \tag{2.1}$$

where

$$\bar{\theta} = \frac{\theta}{\theta_s - \theta_r - (S_1 + S_2)} \tag{2.2}$$

with (originally) fully saturated θ_s and residual θ_r water contents, respectively. The capillary pressure vs. saturation (fundamental relation) we consider in the form

$$\bar{\theta} = \frac{1}{(1 + (\alpha h)^n)^m}, \tag{2.3}$$

where $n > 1$, $m = 1 - \frac{1}{n}$ and $\alpha < 0$ are the soil parameters in the van Genuchten-Mualem (empirical) ansatz (see [1], [4]).
In the saturated zone we have (Darcy's law) $k(h) \equiv 1$. The influence of dynamical viscosity on C_w, S can be found on tables for discrete values of variables and we use a spline interpolation of them in our computations. The Richard's type equation modelling the contaminated suspension flow reads as follows

$$\partial_t \theta + \nabla.(q_w + q_s) + \partial_t(S_1 + S_2) = 0, \tag{2.4}$$

$$\partial_t(\theta C_w) + \nabla.(q_w C_w - \theta \mathbf{D} \nabla C_w) + \rho_m \partial_t S_1 = 0, \tag{2.5}$$

$$\partial_t S_1 = \kappa(\Psi_1(C_w) - S_1), \tag{2.6}$$

$$\partial_t(\theta f) + \nabla.q_s + \partial_t S_2 = 0, \tag{2.7}$$

$$\partial_t S_2 = \Psi_2(S_2)\theta f. \tag{2.8}$$

The suspension flux is

$$\vec{q_0}(x,t) = -K(C_w, S, h)\left(\nabla h - \left(1 - f + f\frac{\rho_s}{\rho_w}\right)e_z\right),\ \bar{\theta} = \frac{\theta}{\theta_s - \theta_r - S_1 - S_2}, \tag{2.9}$$

then the water and silt flux is

$$q_w = (1-f)\vec{q_0},\ q_s = f\vec{q_0} - (1-f)(D_0\theta I + \theta \mathbf{D}).\nabla f, \tag{2.10}$$

where D_0 is molecular difusion coefficient and I is identity matrix.

2.2. Contaminant and silt transport model. The flux of dissolved contaminant with concentration C_w denoted by $\mathbf{J}_{C_w}$ is

$$\mathbf{J}_{C_w} = \theta(\mathbf{v}C_w - \mathbf{D}\nabla C_w). \tag{2.11}$$

Here, $\mathbf{v}$ is the seepage velocity of the contaminated suspension linked with the flux $\vec{q_0} = \mathbf{v}\theta$ in the suspension flow model. Denote by $\mathbf{D}$ the dispersion matrix with the components

$$D_{ij} = (D_0 + \alpha_T|\mathbf{v}|)\delta_{ij} + \frac{v_i v_j}{|\mathbf{v}|}(\alpha_L - \alpha_T),$$

where α_L and α_T are longitudinal and transversal dispersive coefficients, respectively, δ_{ij} is the Kronecker delta and D_0 is the molecular diffusion coefficient. Then, the contaminant transport model is (2.5). The adsorption of the contaminant is governed by the ODE (2.6) (see [1]). The adsorption isotherm Ψ_1 belongs to a chosen class of functions with tuning parameters underlying for determination via solution of corresponding inverse problem.

The conservation of silt in suspension is governed by (2.7) and (2.8). The filtration function also belongs to a chosen class with tuning parameters underlying for determination. We use a simple form $\Psi_2(S_2) = \frac{1}{\bar{a}+\bar{b}S_2}$ with tuning parameters $\bar{a}, \bar{b}$. In solution of inverse problems we consider axially symmetric cylindrical sample and thus we rewrite our model in cylindrical coordinates.

3. Mathematical model in cylindrical coordinates. Our sample is a cylinder with the radius R and the height Z. We transform the mathematical model using cylindrical coordinates (r, z).

3.1. Flow of contaminated water. The governing PDE for infiltration (in gravitational mode) reads as follows

$$\partial_t\theta(h) = \frac{1}{r}\partial_r(rK(C_w,S,h)\partial_r h - (1-f)(D_0\theta + \theta D_{1,1}\partial_r f + \theta D_{1,2}\partial_z f))$$

$$+\partial_z(K(C_w,S,h)(\partial_z h - \xi) - (1-f)(D_0\theta + \theta D_{2,1}\partial_r f + \theta D_{2,2}\partial_z f)) - \partial_t(\rho_m S_1 + S_2),$$

where

$$\xi = 1 - f + f\frac{\rho_s}{\rho_w}.$$

The suspension flux in cylindrical coordinates is of the form

$$\vec{q_0} = -(q^r, q^z)^T, \tag{3.1}$$

$$q^r = K(C_w,S,h)\partial_r h,\ q^z = K(C_w,S,h)(\partial_z h - \xi).$$

3.2. Contaminant transport by water. A matrix $\mathbf{D}$ is of the form

$$\mathbf{D} = \begin{pmatrix} D_{1,1} & D_{1,2} \\ D_{2,1} & D_{2,2} \end{pmatrix} = \begin{pmatrix} \alpha_L(q^r)^2 + \alpha_T(q^z)^2 & (\alpha_L - \alpha_T)(q^r q^z) \\ (\alpha_L - \alpha_T)(q^r q^z) & \alpha_L(q^z)^2 + \alpha_T(q^r)^2 \end{pmatrix} \frac{1}{|\vec{q_0}|}. \tag{3.2}$$

Denote by

$$QC^r = -q^r C_w + \theta(D_{1,1}\partial_r C_w + D_{1,2}\partial_z C_w) + D_o\theta C_w, \tag{3.3}$$

$$QC^z = -q^z C_w + \theta(D_{2,1}\partial_r C_w + D_{2,2}\partial_z C_w) + D_o\theta C_w. \tag{3.4}$$

Then, the contaminant transport reads as

$$\partial_t(\theta C_w) - \left(\frac{1}{r}\partial_r(rQC^r) + \partial_z(QC^z)\right) = -\rho_m\partial_t S_1. \tag{3.5}$$

3.3. Silt transport. We define silt fluxes Qf^r, Qf^z in the same way as QC^r, QC^z, where we replace C_w by f. Then we rewrite the heat transport equation replacing C_w, QC^r, QC^z by f, Qf^r, Qf^z and obtain contaminant transport equation in cylindrical coordinates.

These governing equations are completed by corresponding boundary conditions including the external driven forces. For simplicity, we assume that on the boundary there are prescribed fluxes or values of the unknown h, C_w, f, and a combination of them. Also, water and heat energy transmission from externally driven forces into facade could be considered and the corresponding transmission coefficient could be scaled by the solution of the inverse problem.

4. Numerical method. We approximate the time derivative by backwards difference and then we integrate our system over the angular control volume $V_{i,j}$ with the corners $r_{i\pm1/2}, z_{j\pm1/2}$ and with the length $(\Delta r, \Delta z)$ of the edges. Then, our approximation (by FV method) in the inner grid point (r_i, z_j) at the time $t = t_k$ and used abbreviation $K(U) := K(C_w^{k-1}, S^{k-1}, h)$ is

$$\begin{aligned}
&\frac{\theta(h)-\theta(h^{k-1})}{\tau}\Delta r\Delta z - \Delta z\frac{r_{i+1/2}}{r_i}\left[\frac{K(U_{i+1})+K(U)}{2}\left(\frac{h_{i+1}-h}{\Delta r}\right)\right]\\
&\qquad + \Delta z\frac{r_{i-1/2}}{r_i}\left[\frac{K(U)+K(U_{i-1})}{2}\left(\frac{h-h_{i-1}}{\Delta r}\right)\right]\\
&\qquad - \Delta r\left[\frac{K(U_{j+1})+K(U)}{2}\left(\frac{h_{j+1}-h}{\Delta z}-\xi\right)\right]\\
&\qquad + \Delta r\left[\frac{K(U)+K(U_{j-1})}{2}\left(\frac{h-h_{j-1}}{\Delta z}-\xi\right)\right]\\
&\qquad = -\left(\frac{S_1^k-S_1^{k-1}}{\tau}+\frac{S_2^k-S_2^{k-1}}{\tau}\right)\Delta r\Delta z
\end{aligned} \tag{4.1}$$

where only changes of $\{i, j\}$ are indicated.

4.1. Quasi-Newton linearisation. In each (r_i, z_j) we linearise θ in terms of h iteratively (with iteration parameter l) following [3] in the following way

$$\frac{\theta(h^{k,l+1})-\theta(h^{k-1})}{\tau} = R^{k,l}\frac{h^{k,l+1}-h^{k,l}}{\tau}+\frac{\theta^{k,l}-\theta^{k-1}}{\tau}, \tag{4.2}$$

where

$$R^{k,l} = \frac{\partial\theta^{k,l}}{\partial h^{k,l}} = (\theta_s-\theta_r-S_1-S_2)(1-n)\alpha(\alpha h^{k,l})^{n-1}(1+(\alpha h^{k,l})^n)^{-(m+1)}$$

for $h^{k,l} < 0$, else $R^{k,l} = 0$. We stop iterations for $l = l^*$, when $\left|h^{k,l^*+1}-h^{k,l^*}\right| \le$ *tolerance* and then we put $h^k := h^{k,l^*+1}$. Finally, we replace the non-linear term $K(U^k)$ by $K(U^{k,l})$, then our approximation scheme becomes linear in terms of $h^{k,l+1}$. Generally, we speed the iteration by the special construction of starting point $h^{k,0} \approx h^{k-1}$, and using suitable damping parameter in solving the corresponding linearized system. Applying operator splitting method in successive solution for adsorption and deposition at the time section $t = t_k$ we start from $t = t_{k-1}$ and use the obtained flow characteristics from $t = t_k$ for $\theta^k, h^k, \vec{q}^k$ and for matrix $\mathbf{D}^k$. We use the same

approximation strategy for the transport of silt and contaminant. To obtain approximation linked with the boundary points we apply the same strategy of the finite volume method, where the control volume $V_{i,j}$ is only half or quarter of the $\Delta r \Delta z$ corresponding to the inner grid points. All iterations we realize in the flow part of the model thanks to the operator splitting strategy. The other model variables are taken from the time section $k-1$. The approximation of other model equation is very similar and must be done carefully for flux $\vec{q_0}$ and matrix $\mathbf{D}$.

5. Inverse problems. The determination of parameters $K_s, n, \alpha, \alpha_L, \alpha_T$ we have discussed in our previous contributions (see [5]).

We shortly discuss the determination of adsorption function Ψ_1 with the kinetic rate coefficient κ and the filtration function Ψ_2. We use the following experimental scenario. The sample cylinder is flow isolated on the top. The cylinder mantel is immersed in the bigger cylinder with contaminated suspension with concentration $C_w = 0.035$. The sample is dry $h = -200$. On the sample boundary, hydrostatic pressure is affected by the suspension. The suspension level is originally with the height H above the top of the sample, see Fig 1.1. We measure the time evolution of the cumulated outflow concentration which is our characteristics for the inverse problem method. The outflow proceeds through the sample bottom with half radius ($R_1 = R/2$). In our experiment we use the adsorption with Langmuir isotherm $\Psi_1(C_w) = \frac{aC_w}{b+C_w}$, where {a,b} are tuning parameters underlying for determination. We use the computed characteristics with the starting model parameter $p_s = [a, b, \kappa]$. Then, we add some noise to the computed characteristics (representing measured characteristics) and forget the used model parameters. Iteratively we compute the optimal model parameters minimizing the discrepancy of computed and measured characteristics.

These optimal parameters we consider as required model parameters in our complex model. The obtained model parameters are collected in the Tab 5.1 together with the starting points used in the iteration procedure. The computed and modified characteristics with noise are drawn in the Fig. 5.1.

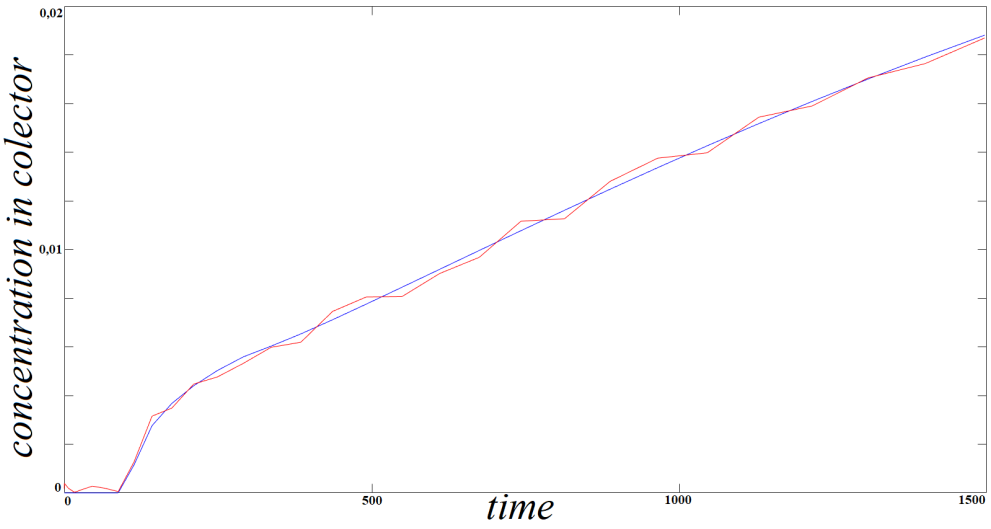

FIG. 5.1. *Time evolution of the contaminant concentration of the cumulated suspension in the outflow chamber (blue) and with random noise (red)*

We test the reliability of the obtained model parameters by choosing different starting parameters in the iteration procedure and changing the level of added noise. These facts and the sensitivity of characteristics on model parameters create the ground for suitability of suggested experimental scenario.

TABLE 5.1
Optimal values of a, b, κ *for* $p_s = [2, 1, 0.05]$ *with noise* 0.01

p_{start}	p_{opt}
$[1, 0.5, 0.01]$	$[1.9901, 0.9484, 0.04934]$
$[1, 0.5, 0.01]$	$[1.9319, 0.9398, 0.05069]$
$[3, 0.5, 0.01]$	$[2.0059, 1.0529, 0.05099]$
$[3, 0.5, 0.01]$	$[2.0774, 1.0515, 0.04929]$
$[1, 2, 0.01]$	$[1.9904, 1.0384, 0.05024]$
$[1, 2, 0.01]$	$[1.9943, 0.9523, 0.04971]$
$[3, 2, 0.01]$	$[2.0555, 1.0427, 0.04930]$
$[3, 2, 0.01]$	$[1.9226, 1.0558, 0.04976]$
$[1, 0.5, 0.1]$	$[1.9303, 1.0381, 0.05010]$
$[1, 0.5, 0.1]$	$[1.9190, 1.0596, 0.04943]$
$[3, 0.5, 0.1]$	$[1.9801, 0.9355, 0.04907]$
$[3, 0.5, 0.1]$	$[1.9697, 1.0707, 0.04982]$
$[1, 2, 0.1]$	$[1.9493, 1.0306, 0.05079]$
$[1, 2, 0.1]$	$[1.9372, 1.0650, 0.05028]$
$[3, 2, 0.1]$	$[1.9214, 0.9552, 0.04981]$
$[3, 2, 0.1]$	$[2.0414, 1.0373, 0.04969]$

The determination of model parameters for the function $\Psi_2(S_2) = \frac{1}{\bar{a}+bS_2}$ proceeds in a similar way. Here in the outer cylinder, we use the suspension with a given constant fraction $f = 1/3$. On the outflow, we measure the silt fraction evolution of cumulated outflow suspension.

6. Direct solution of our complex model. Finally, we present the solution of the complex system with suspension flow, silt deposition and also with contaminant adsorption. We will use the following model data ([CGS]) $\theta_0 = 0.38$, $\theta_r = 0$, $K_s = 2.4\ 10^{-4}$, $\alpha = 0.0189$, $n = 2.81$, $g = 981$, $H(0) = 5$, $D_0 = 0.01$, $\alpha_L = 1$, $\alpha_T = \frac{1}{10}$, $c_v = c_m = 1$,$\kappa = 0.05$, $\rho_m = 1$, $a = 2, b = 1$, $\Psi_2(S_2) = \frac{1}{150+300S_2}$. The Ψ_2 function is rather an intensive filtration function, which stops the infiltration in a relatively short time. In Fig. 6.1, Fig. 6.2 and Fig. 6.3 we present the evolution of pressure head, effective saturation, silt fraction in suspension, deposited silt, contaminant concentration in suspension, and adsorbed contaminant in 3 time sections. We use $t_1 = 30s$, $t_2 = 250s$, $t_3 = 813s$. The used parameters in the filtration function cause the quick filling of the pores by the deposited silt near the infiltration boundary. In this case, the continuation of the infiltration process stopped after a short time. Inside the sample, there is a redistribution of the saturation leaving part of the sample suspension free as you can see in Fig. 6.3. Moreover we include figures with level contours of h,$\theta_e f$,f and S_2 in the corresponding time sections as we can see in Fig. 6.4. For time $t = 30s$ we use a red dashed line, for time $t = 250s$ we use a blue dash-dotted line and for time $t = 813s$ we use a green solid line.

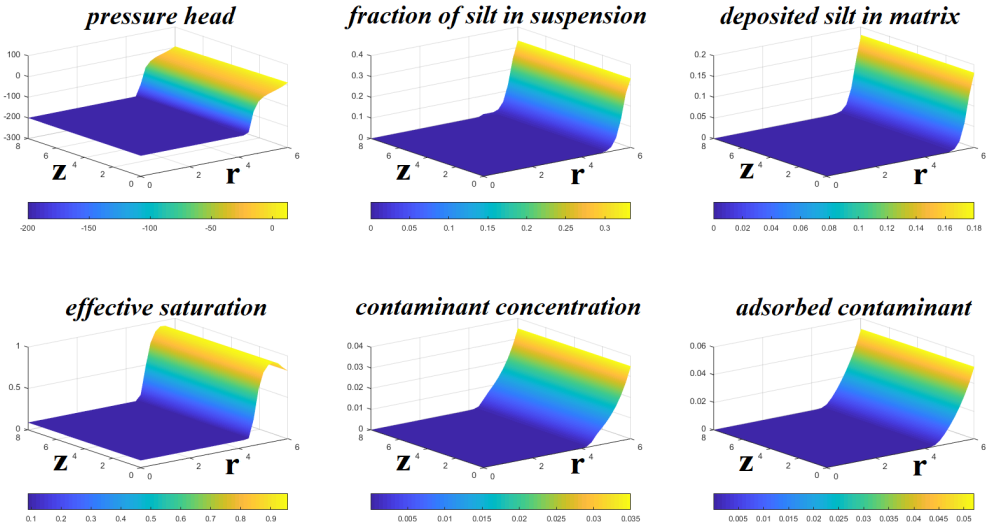

FIG. 6.1. *Distribution of the entity values inside the sample at the time* $t = 30s$.

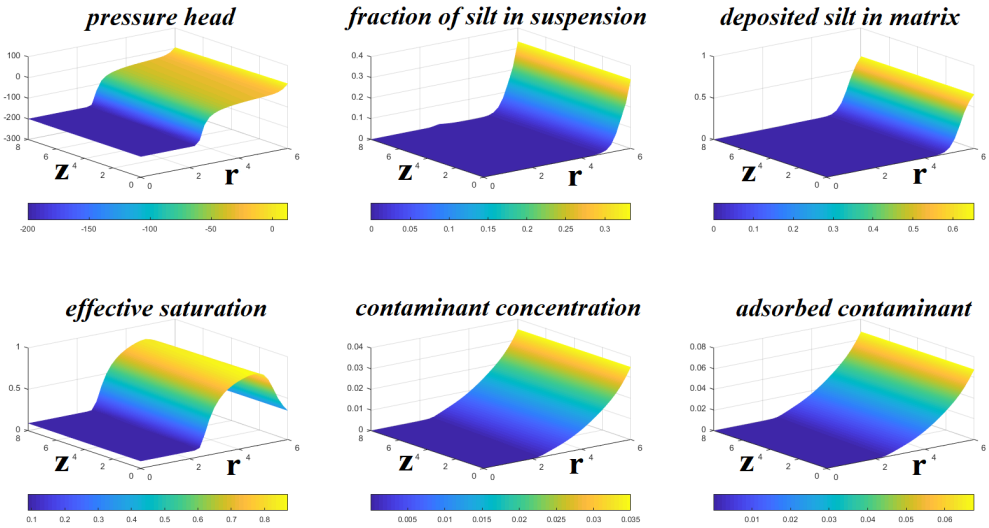

FIG. 6.2. *Distribution of the entity values inside the sample at the time* $t = 250s$

7. Summary. Numerical modeling of contaminated suspension infiltration into unsaturated porous media is discussed. The mathematical model includes silt and contaminant transport with silt deposition and contaminant adsorption.

The adsorbed contaminant, deposited silt, and adsorbed contaminant influence the hydraulic permeability and degrades the porosity.

The efficient numerical method is developed on the base of operator splitting, flexible time discretization, and finite volume method. In our numerical experiments, we have demonstrated the suitability of the proposed method for solving direct and inverse problems. A laboratory experiment scenario is proposed to determine the adsorption and filtration functions and rate coefficient of adsorption.

In the direct solution of our complex model, we demonstrated the correctness and

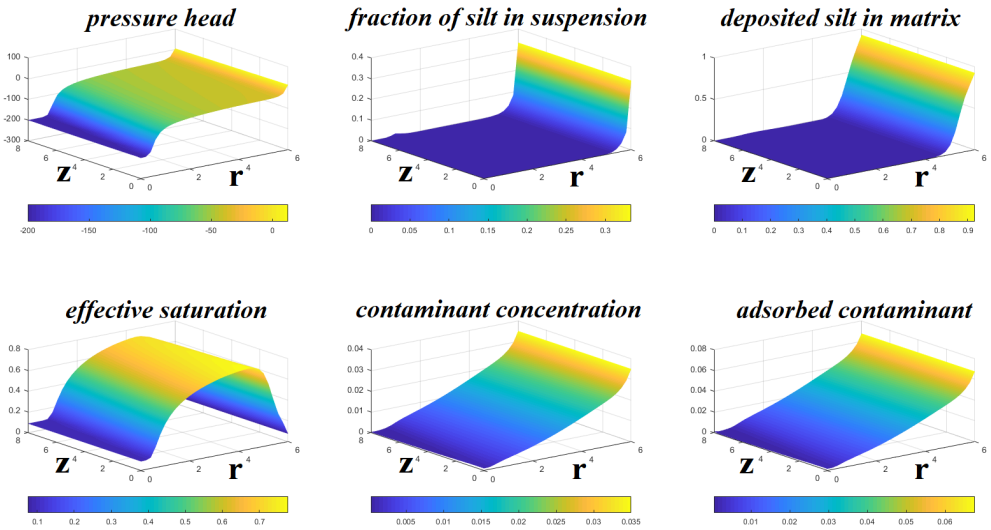

FIG. 6.3. *Distribution of the entity values inside the sample at the time* $t = 813s$

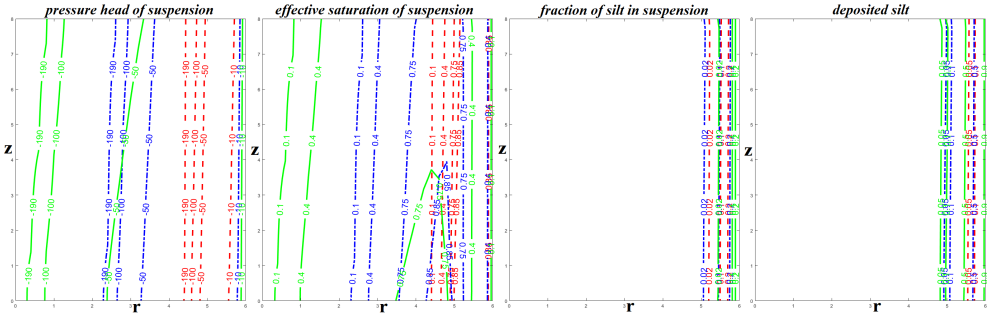

FIG. 6.4. *Time evolution of the contours for* $t = 30s$ *red dashed line, for* $t = 250s$ *blue dash-dotted line and for* $t = 813s$ *green solid line*

efficiency of our numerical method for solving the direct and inverse problem.

Acknowledgments. The authors confirm financial support by the Slovak Research and Development Agency under the contracts APVV-15-0681.

REFERENCES

[1] J. BEAR AND A. H.-D. CHENG, *Modeling Groundwater Flow and Contaminant Transport*, Springer, V.23, (2010).

[2] J. ŠIMUNEK, M. ŠEJNA, H. SAITO, M. SAKAI AND M. TH. VAN GENUCHTEN, *The Hydrus-1D Software Package for Simulating the Movement of Water, Heat, and Multiple Solutes in Variably Saturated Media*, Riverside, California (2008).

[3] M. A. CELIA AND Z. BOULOUTAS, *A general mass-conservative numerical solution for the unsaturated flow equation*, Water Resour. Res. 26 (1990), p. 1483–1496.

[4] M.T. VAN GENUCHTEN, *A closed-form equation for predicting the hydraulic conductivity of unsaturated soils*, Soil science society of American Journal, vol 44, (1980), p. 892-898.

[5] J. KAČUR, P. MIHALA AND M. TÓTH, *Determination of soil parameters in hydraulic flow model for porous media*, International journal of mechanics, Vol. 11, (2017), p. 36–42.

[6] J. KAČUR AND J. MINÁR, *A benchmark solution for infiltration and adsorption of polluted water into unsaturated-saturated porous media*, Transport in porous media, vol. 97, (2013),

p. 223–239.
[7] T. L. Bergman, A. S. Lavine, F. P. Incropera and D. P. Dewitt, *Fundamentals of heat and mass transfer*, John Wiley and Sons, 7th edition, (2011).
[8] M. Koniorczyk and D. Gawin, *Heat and moisture transport in porous building materials containing salt*, Journal of building physics, vol. 31, no. 4, (2008), p. 279-300.
[9] N.-Z. Sun, *Inverse problems in Groundwater modelling.*, Kluwer, Academics. Dordrecht, (1994).
[10] N.-Z. Sun and A. Sun, *Mathematical Modeling of Groundwater Pollution*, Springer-Verlag, New York, (1996).
[11] A.C. Alvarez, G.Hime, J.D.Silva and D.Marchesin, *Analytic regularization of an inverse filtration problem in porous media*, Inverse Problems 29, (2013).
[12] Z.Mesticou, M.Kacem and PH.Dubujet, *Flow of suspensions through porous media - application to deep filtration*, Indust.Eng.Chem. 65, (1970), p. 8–35.
[13] J.P.Herzig, D.M.Leclerc and P.L.Golf, *Krylov subspace methods for solving large unsymmetric linear systems*, Math. Comp., 37 (1981), pp. 105–126.
[14] P. Bedrikovetsky et al., *Particle detachment under velocity alternation during suspension transport in porous media*, Transport in Porous Media volume 91, (2012), 173–197.
[15] J. Kačur, P. Mihala and M. Tóth, *Numerical modeling of heat exchange and unsaturated-saturated flow in porous media*, Computers and Mathematics with Applications, Vol. 77, No. 9 (2019), pp. 1668–1680.